Solvent Effects on the Surface Composition of Bisphenol A Polycarbonate and Polydimethylsiloxane (BPAC−PDMS) Random Block Copolymers

Hengzhong Zhuang and Joseph A. Gardella, Jr.*

Department of Chemistry, State University of New York at Buffalo, Buffalo, New York 14260-3000

Received July 30, 1996; Revised Manuscript Received January 31, 1997[⊗]

ABSTRACT: The surface compositions of bisphenol A polycarbonate and poly(dimethylsiloxane) (BPAC−PDMS) random block copolymers were analyzed using angle-dependent electron spectroscopy for chemical analysis (ESCA) and attenuated total reflection (ATR) FTIR. The composition was measured at sampling depths of 18, 73, and 103 Å with angle-dependent ESCA and at a sampling depth of 4.1 μm with ATR-FTIR. The present study focuses on examining the quantitative effects of solvent casting and annealing on the surface composition of the BPAC−PDMS random block copolymers of varying bulk compositions. The effects of solvent casting were evaluated in terms of solvent solubility (or Hildebrand parameter) and solvent volatility (or boiling point). It was found that the casting solvents and annealing treatments influenced the surface compositions significantly, and each of the solvents gave the polymer film a different morphology in the near surface region. In addition, a physical picture of the near surface region (103 Å) of siloxane block copolymers cast from selected solvents is compared to the thicker region (∼4.1 μm) probed by ATR-FTIR.

Introduction

We have been concerned with quantitative analysis of the surface composition of siloxane-based multicomponent polymers for some time. The polymer surface of this sort is encountered in some important technologies including minimal fouling coatings[1] and biocompatible cardiovascular materials, where surface excess of a low surface energy component is involved. It has been well established that surface composition and morphology play a crucial role in determining the effectiveness in these applications. This has, in return, prompted extensive studies on many variations which could lead to desired or controlled surface compositions and morphologies. These variations include, but are not limited to, component, architecture, bulk composition, block length, crystallinity, and processing conditions. In our laboratory and others, various poly(dimethylsiloxane) (PDMS)-containing copolymers, such as copolymers of PDMS and polystyrene (PS),[2,3] copolymers of poly(α-methylstyrene) (PMS) and PDMS,[4] poly(tetramethyl-*p*-silphenylenesiloxane)−PDMS multiblock copolymers,[5] copolymers of PDMS and nylon-6,[6] copolymers of bisphenol A polycarbonate and PDMS,[7−9] etc., have been explored. Studies of polymer blends containing PDMS[1,10,11] were also reported. These studies reveal that polymers with different components and bulk compositions have major influences on the surface composition and morphology, as well as the domain structure in the bulk, and the effects of block length, architecture,[3] and crystallinity[5,6] of block copolymers are also found very prominent.

As a processing variation, casting solvents also play an important role in influencing the surface morphology and composition of a multicomponent polymer. Grobe *et al.*[12,13] have studied Biomer extracts and extracts from Cardiothane-51 cast from varying polarity solvents in an attempt to evaluate the surface composition and morphology with angle-dependent electron spectroscopy for chemical analysis (ESCA) and ATR-FTIR. Using angle-dependent ESCA and a concentration depth profile deconvolution program,[14,15] we have investigated effects of casting solvent on the surface compositions of a series of poly(dimethylsiloxane)−urethane−urea copolymers.[16]

Because of the characteristics of low surface energy contributed by PDMS component and excellent mechanical strength and good adhesion to metal substrates provided by bisphenol A polycarbonate (BPAC), the BPAC−PDMS copolymers are one attractive system being studied as potential minimal fouling coatings. In fact, much work has been done on these copolymers. Surface segregation of PDMS (the lower surface energy component) in BPAC−PDMS block copolymers have long been observed.[7−9] Schmitt *et al.*[9] have demonstrated surface segregation of PDMS within a surface layer of a few tens of angstroms, as measured with electron spectroscopy for chemical analysis (ESCA) and within only the top 3−5 Å of the surface,[17] as measured with ion-scattering spectroscopy (ISS) in BPAC−PDMS block copolymers with varying compositions. Mittlefehldt[18] has studied the composition in the near surface region of over 1 μm thick with attenuated total reflection (ATR) FTIR. Chen *et al.*[10] have examined the effects of different PDMS block length on the surface composition of BPAC−PDMS block copolymers.

The present study focuses on the effects of casting solvents on the surface morphology and composition of the BPAC−PDMS random block copolymers. For the BPAC−PDMS random block copolymers with an average of 20 DMS repeat units, the composition of the topmost layer (a few tens of angstroms thick) of the solvent-cast films could be most sensitive to the casting solvent and subsequent annealing treatment. Therefore, we are mainly interested in understanding such regions. ESCA has been established as an effective tool to probe an air−polymer interface of a few tens of angstroms thick. In particular, angle-dependent ESCA with Mg $K\alpha_{1,2}$ as an X-ray source is capable of achieving different sampling depth ranging from a few to approximately 100 Å. As a result, it was used in this work

* To whom correspondence should be addressed.
[⊗] Abstract published in *Advance ACS Abstracts,* May 15, 1997.

S0024-9297(96)01138-2 CCC: $14.00

Scheme 1. Molecular Structure of BPAC−PDMS Copolymers

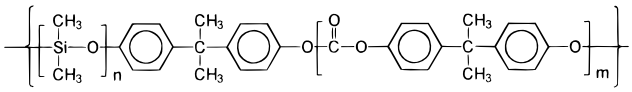

Table 1. Some Properties of Solvents Used To Cast Copolymer Films

solvent	CCl_4	C_4H_8O	C_6H_6	$CHCl_3$	CH_2Cl_2	C_5H_5N
δ/MPa$^{1/2}$ [a]	17.6	18.6	18.8	19.0	19.8	21.9
bp °C	76.7	66.0	80.1	61.1	39.8	115.0

[a] δ/MPa$^{1/2}$: Hildebrand parameter of liquid at 25 °C.

as a primary tool for investigating solvent and annealing effects on the surface composition of BPAC−PDMS copolymers. In addition, ATR-FTIR, capable of sampling a few micrometers in depth, was employed as a complementary technique to examine the composition at a much greater depth.

Experimental Section

Materials and Preparation. The random block copolymers of BPAC and PDMS were provided by Dr. Roger Kambour from General Electric Co., Schenectady, NY. All polymers were used as received. The structure of the polymer is shown in Scheme 1. They have an average PDMS block length of 20 DMS repeat units and the following weight percent compositions: 35/65, BPAC−PDMS; 50/50, BPAC−PDMS; and 75/25, BPAC−PDMS.[10,19] Six solvents with distinctive properties (see Table 1) were selected, in particular, carbon tetrachloride (100% by GC, corrected for H_2O, J. T. Baker Chemical Co., Phillipsburg, NJ), tetrahydrofuran (GR, Fisher Scientific, Pittsburgh, PA), benzene (GR, EM Science, Gibbstown, NJ), chloroform (99.9%, Fisher Scientific, Pittsburgh, PA), methylene dichloride (99.9%, Fisher Scientific, Pittsburgh, PA), and pyridine (99.9+%, HPLC Grade, Aldrich Chemical Co., Milwaukee, WI). They were used as received. The PDMS homopolymer is a secondary standard with MW = 93 700. The BPAC homopolymer is also a secondary standard with MW = 38 400. Both of them were purchased from Scientific Polymer Products, Inc. (Webster, NY).

All samples for ESCA measurements were cast as films in clean aluminum weighing pans from *ca.* 0.5% (w/v) solutions in those six solvents, respectively. The films were allowed to air-dry at room temperature for over 72 h. One-half of the samples were analyzed without any further treatment; the other half were annealed at 180 °C for 17 h in a vacuum oven before being analyzed. The selection of an annealing temperature of 180 °C is justified by the fact that the glass transition temperature of BPAC homopolymer is 149 °C,[20] and thus the glass transition temperature of a BPAC−PDMS copolymer should be below this value. Such a harsh annealing condition was used to ensure the films to attain a thermodynamic equilibrium. It has been reported that no residual solvent in the polymer films is detectable by ESCA with a detection limit of less than 1 atom % through the above sample preparation.[4]

The samples for ATR-FTIR measurements were prepared in the same way as those for ESCA measurements. For transmission (TX) FTIR experiments, copolymer solution of *ca.* 1% (w/v) in chloroform was deposited directly onto clean KBr plates. The samples were then air-dried overnight. The thickness of the resultant film for TX-FTIR measurements was controlled so that the IR absorbance was between 0.3−1.0 at the maximum absorption peak.

Instrumentation. Angle-dependent ESCA spectra were acquired on a Perkin-Elmer Physical Electronics Model 5300 ESCA spectrometer with a hemispherical analyzer and a single-channel detector. Mg $K\alpha_{1,2}$ X-rays were used as the source, operated at 300 W (15.0 kV and 20 mA). The base pressure in the main chamber was maintained at $\leq 5.0 \times 10^{-8}$ Torr. Prior to the high-resolution ESCA spectrum acquisition for each sample, an ESCA survey spectrum with the binding energy ranging from 0 to 1000 eV was recorded at a rate of

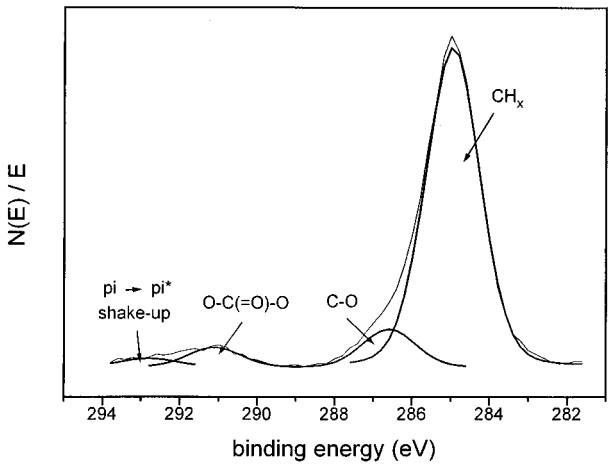

Figure 1. A least-squares curve fitting of the ESCA spectrum of the BPAC−PDMS (75/25) copolymer cast from methylene dichloride measured at 90° takeoff angle, the thin line represents the experimental spectra without being smoothed and the thick line represents the curve fit.

Table 2. Peak Components Used in the Curve Fitting of Figure 1

peak components	CH_X	C−O	O−C(=O)−O	$\pi \rightarrow \pi^*$
position estimate (eV)	285.00	286.64	291.14	292.74
intensity estimate (counts, eV/s)	35681	4193	2160	915
fwhm estimate (eV)	1.65	1.60	1.57	1.70
Gaussian estimate (%)	85	95	95	95

1.000 eV/step and a takeoff angle of 45° with a pass energy of 89.45 eV. A pass energy of 35.75 eV and a rate of 0.200 eV/step were used for all the high-resolution ESCA spectrum acquisitions with a binding energy window of 20 eV. High-resolution spectra of carbon 1s (C1s), oxygen 1s (O1s), and silicon 2p (Si2p) core levels for each sample were acquired at takeoff angles of 10°, 45°, and 90°, respectively. This led to corresponding sampling depths of approximately 18, 73, and 103 Å.[21] No radiation damage was observed during twice the regular data acquisition time duration, as evidenced from no change in the ESCA spectra and no decolorations. ESCA data manipulation was performed using a Perkin-Elmer 7500 computer running a PHI ESCA version 2.0 software.[22]

Both TX-FTIR and ATR-FTIR experiments were conducted on a Nicolet Magna-IR 550 spectrometer with a DTGS detector at a resolution of 4 cm^{-1}. For collections of TX-FTIR and ATR-FTIR spectra, 16 and 100 scans were ran respectively. Being mounted on a Harrick Scientific Model X ATR attachment, a Harrick Ge prism (50 × 10 × 3 mm^3) with a face cut at 45° was used as the internal reflectance element for all the ATR-FTIR measurements. An incident analysis angle of 45° was chosen to yield a penetration depth (d_p) of 1.37 μm and a resultant sampling depth ($3d_p$) of approximately 4.1 μm[18] from the free surface at an incident wavelength of 8.33 μm (1200 cm^{-1}).

Analysis of Experimental Results

ESCA Results. Photoelectrons assigned to carbon 1s, oxygen 1s, and silicon 2p core levels were detected in ESCA spectra of the BPAC−PDMS copolymers. The C1s peak, in particular, could be used to perform quantitative analysis of these copolymers because of the characteristic chemical shift of C1s peak originated from BPAC component. Figure 1, for instance, is a C1s spectrum of the BPAC−PDMS (75/25) copolymer cast from methylene dichloride solution (~0.5% (w/v)) measured at 90° takeoff angle and its least-squares computer fit comprising C1s photoelectrons from CH_X, C−O, O−C(=O)−O and $\pi \rightarrow \pi^*$ shake-up (Table 2). C1s peaks for C−O, O−C(=O)−O and $\pi \rightarrow \pi^*$ shake-up are

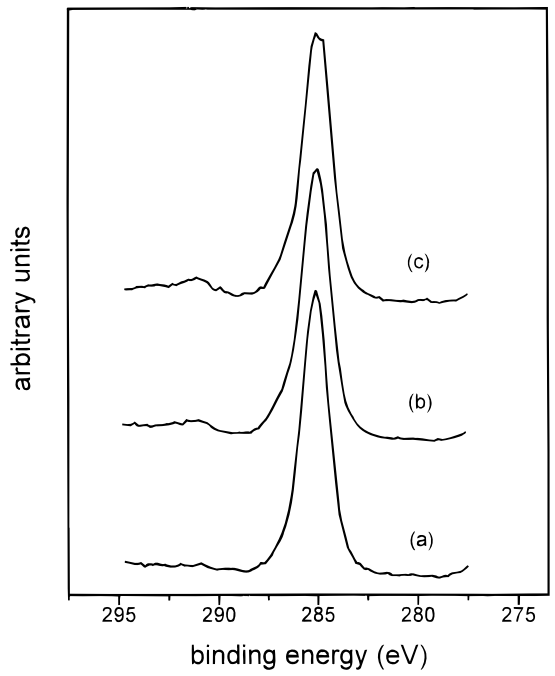

Figure 2. C1s spectra of the BPAC−PDMS (75/25) copolymer cast from methylene dichloride measured at (a) 10°, (b) 45°, and (c) 90° takeoff angles.

contributed solely by BPAC, while the C1s peak for CH_X is contributed by both BPAC and PDMS. This is illustrated by the fact that the ratio of the C−O peak to the O−C(=O)−O peak is 2:1, which is the ratio in the BPAC monomer. By computing the relative intensity of, for instance, the C1s peak for C−O or O−C(=O)−O characteristic of BPAC *versus* that for CH_X contributed by both BPAC and PDMS, it is possible to evaluate the compositional percentages of BPAC and PDMS in the copolymer. Schmitt *et al.*[9] have utilized this method for quantifying the surface composition of BPAC−PDMS copolymers. But in their work, ESCA spectra were recorded at large takeoff angles (≥15°) using a cylindrical mirror analyzer which detects signals at a larger acceptance angle. As a result, deeper surface layers were probed and greater concentrations of BPAC were observed.

However, the signal of C1s photoelectrons from either C−O, or O−C(=O)−O, or $\pi \rightarrow \pi^*$ shake-up would be too weak for quantification if recorded at shallow angles due to the surface segregation behavior of PDMS. This argument is evidenced by the ESCA spectrum of the BPAC−PDMS (75/25) copolymer cast from methylene dichloride at 10° takeoff angle, as shown in Figure 2a, in which the C1s peak for O−C(=O)−O (~291.2 eV) is remarkably weak. Figure 2a−c are the C1s spectra acquired at takeoff angles of 10°, 45°, and 90°. A trend is observed from the change of the peak intensities of C1s photoelectrons due to C−O, O−C(=O)−O, and $\pi \rightarrow \pi^*$ shake-up in Figure 2. Specifically, the percentage of PDMS increases while that of BPAC decreases from at 90° to 45° and almost diminishes at 10°.

To circumvent the difficulty in quantifying the spectra at shallow takeoff angles by curve fitting, an alternative method has to be utilized here. The rationale of this method[3,20] is as follows. Si is selected to label PDMS component in the copolymer, and the intensity of Si2p peak is used to monitor the relative concentration of PDMS. Although there is no unique element which could be suitable for unambiguously labeling BPAC, the concentration of BPAC in the copolymer can be indirectly computed by subtracting the C1s peak component attributed to CH_X in PDMS from the total C1s peak attributed to CH_X in both BPAC and PDMS, C−O and O−C(=O)−O in BPAC. Assume that if one Si atom is observed, the whole repeat unit of PDMS

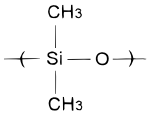

will be present at a given sampling depth; and if 16 carbon (C) atoms from BPAC are observed at the same time, the whole repeat unit of BPAC

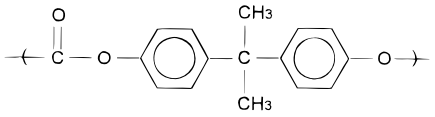

7

will be present at that same sampling depth. This assumption is based on the fact that the kinetic energies of electrons emitted from Si2p core-levels and of those emitted from C1s core-levels are of the same magnitude, it is therefore not necessary to correct for the difference in inelastic mean free path as it is when quantitating with electrons emitted from different elements. As a result, Si2p and C1s peaks were integrated and ratioed (Si/C), and then calculated in the following way. Since there are two carbon atoms and one silicon atom in a PDMS repeat unit (MW = 74.2), and 16 carbon atoms but no silicon in each BPAC repeat unit (MW = 254.3) ideally, the overall atomic concentration ratio of silicon to carbon (Si/C) ranges from 0 (the surface region occupied by BPAC exclusively) to $^1/_2$ (the surface region occupied by PDMS exclusively). It reflects the relative amounts of the two components in the surface region of BPAC−PDMS block copolymers. If X represents the molar fraction of PDMS, $(1 - X)$ will be the molar fraction of BPAC in the BPAC−PDMS copolymer, and Si/C atomic ratio can be, theoretically, formulated as

$$\frac{\text{Si}}{\text{C}} = \frac{X}{2X + 16\,(1 - X)} \tag{1}$$

Furthermore, if W represents the weight fraction of PDMS in the copolymer, the above equation can be transformed as

$$\frac{\text{Si}}{\text{C}} = \frac{W/74.2}{2W/74.2 + 16(1 - W)/254.3} \tag{2}$$

Therefore, from the atomic percentage data obtained with the PHI version 2.0 ESCA software, mass percentages of PDMS were calculated and used throughout this paper

$$W(\%) = \frac{1187.2\ (\text{Si/C})}{254.3 + 678.6\ (\text{Si/C})} \times 100 \tag{3}$$

This method also has the weakness of not being able to quantify very small amounts of BPAC (or PDMS) at the surface because of the elemental detection limit in ESCA measurements.

IR Results. ATR-FTIR was used to determine compositions at a much greater depth. Because the sampling depth in ATR-FTIR measurements is directly proportional to the incident wavelength,[23] it is necessary

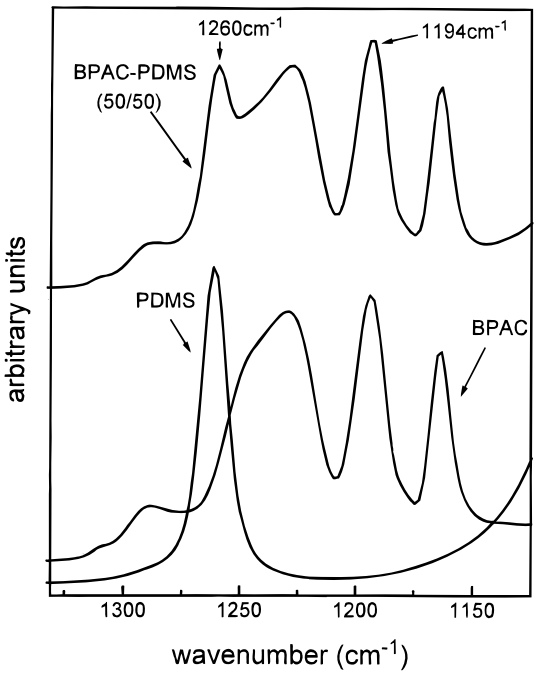

Figure 3. An ATR-FTIR spectrum of the BPAC−PDMS (50/50) copolymer, compared with TX-FTIR spectra of pure BPAC and PDMS.

to choose one peak for each component; the two peaks should be as close as possible to quantify a two component system. For example, the sampling depth approaches 4.1 μm at 45° incident angle with 45° face-cut Ge prism at an incident wavelength of 8.33 μm (equivalent to 1200 cm^{-1}).[23] Figure 3 (upper trace) is a segment of a typical ATR-FTIR spectrum of the BPAC−PDMS copolymer, compared with transmission IR spectra (lower traces) of pure PDMS and BPAC. The peak at 1260 cm^{-1} indicative of PDMS overlaps with a neighboring band from BPAC (Figure 3, upper trace). To quantify the PDMS relative concentration in the copolymer, the peak at 1260 cm^{-1} has to be separated and ratioed to its proximate peak at 1194 cm^{-1} indicative of BPAC. The reason for choosing the peak 1194 cm^{-1} instead of the one at its right (at ∼1160 cm^{-1}) to characterize BPAC is that the former is closer to the peak at 1260 cm^{-1} indicative of PDMS and also happens to be the strongest one resulting from BPAC. There are several ways to separate the peak at 1260 cm^{-1}, including Fourier deconvolution (FD),[18,19,24−26] maximum likelihood restoration,[27] and curve fitting.[28] We chose Fourier deconvolution toward this end since maximum likelihood restoration does not recover peaks completely and curve fitting necessitates knowledge of the number of component peaks and their positions to obtain a good result.

In the present work, FD was accomplished with Asystant (ASYST Software Technology, Inc. Rochester, NY) developed from within the intrinsic programming language of ASYST. This routine was developed by Mittlefehldt[18] the basis of the work by Kauppinen *et al.*[24−26] Unlike commercial FD programs, the mathematical functions and parameters in this program can be controllably changed. For example, the Lorentzian function

$$E_o(\nu) = \frac{\sigma/\pi}{\sigma^2 + (\nu - \nu_o)^2} \qquad (4)$$

was selected as the filter function, and

$$\mathrm{Sinc}^2 = \frac{\sin X}{X} \qquad (X \neq 0) \qquad (5)$$

was screened out as the apodization function. These two mathematical functions were programmed in ASYST language. 128 (2^N) data points (from about 1330 to 1085 cm^{-1}) truncated from an entire measured IR spectrum (with resolution of 4 cm^{-1}) was selected for carrying out Fourier deconvolution. Different fwhh values (2σ) of the filter function (refer to eq 4) and apodization function widths (the interval between the upper and lower limits of X values in eq 5) were tried. Through trial and error, σ of 3.2 data points and apodization function width of 32 data points were screened out as optimal values and used throughout the entire study. As an example, Figure 4 illustrates the deconvoluted ATR-FTIR spectrum (lower trace) of the BPAC−PDMS (50/50) copolymer, using the optimized parameters. It represents a fairly well deconvoluted spectrum. This Fourier deconvolution program has been discussed in greater detail in refs 18, 19, and 29.

After the IR spectra were deconvoluted with this Fourier deconvolution program, the peak at 1260 cm^{-1}, characteristic of PDMS, was integrated and ratioed to the peak at 1194 cm^{-1}, characteristic of BPAC (Figure 4). To obtain the concentration of PDMS, a compositional calibration curve was established from seven deconvoluted transmission IR spectra of BPAC/PDMS blends of known compositions.[29] The PDMS surface concentration of the copolymers were quantified subsequently from the ATR-FTIR measurements, and the errors in the PDMS concentrations measured by this method are less than ±3% by weight. It is worth noting that the weight percentage of PDMS obtained is an average value over the entire detection range (∼4.1 μm).

Discussion

Structural and Compositional Influence on Surface Enrichment of PDMS. We have previously studied this polymer series by ESCA[9,20] and ATR-FTIR[19] in an effort to evaluate surface composition at various depths. The present study includes results of these polymers cast from chloroform, a typical casting solvent used in previous studies. A short discussion of the present results and comparison to previous work are given to set a context for the study of solvent effects.

Random block copolymers, such as the BPAC−PDMS copolymers, in which both block A and B are polydisperse, exhibit a morphology that is generally less ordered than other types of block copolymers. PDMS tends to segregate and remain in the air−polymer interface since it has a lower surface energy (21 mN/m)[10] compared to BPAC (43 mN/m)[10] in the BPAC−PDMS copolymers. This is exemplified by Figure 5, a plot of surface concentrations (in the topmost 18 Å) of PDMS *versus* PDMS content in the bulk. The surface enrichment of PDMS within the topmost 18 Å layer (cast from chloroform) is remarkable with respect to the bulk concentration of the BPAC−PDMS 35/65, 50/50, and 75/25 copolymers, respectively. Within the topmost 18 Å, the weight percentage of PDMS is nearly the same within error limit for the BPAC−PDMS (35/65) and the BPAC−PDMS (50/50) copolymers; both have a higher weight percentage of PDMS than does the BPAC−PDMS (75/25) copolymer. This observation means that increasing the PDMS content in the bulk will definitely increase the PDMS concentration in the topmost 18 Å layer; however; this trend soon plateaus, although

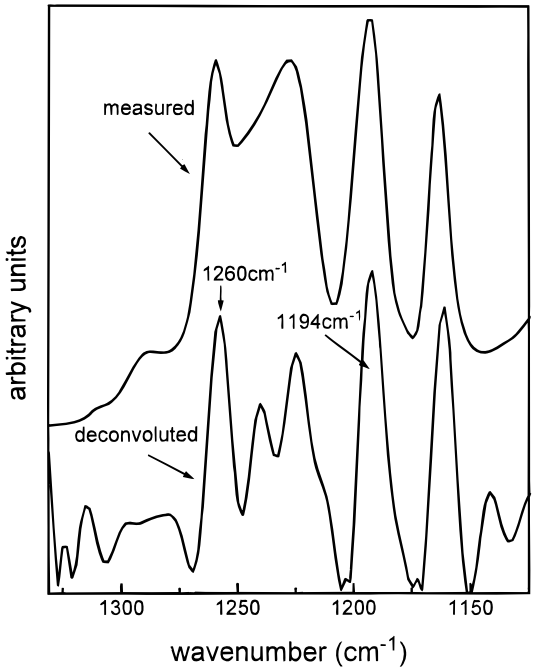

Figure 4. A deconvoluted ATR-FTIR spectrum of the BPAC−PDMS (50/50) copolymer, compared with the measured one.

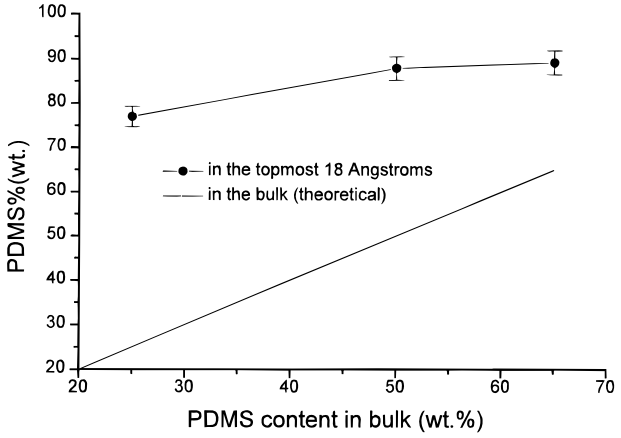

Figure 5. PDMS surface enrichment in the topmost 18 Å of the BPAC−PDMS copolymers cast from chloroform.

PDMS continues to enrich in deeper surface regions with increasing PDMS content in the bulk.

McGrath *et al.*[7] and Dwight *et al.*[8] have also shown such surface segregation of PDMS in BPAC−PDMS copolymers. They found that the surface was nearly pure siloxane over a narrow concentration range near 50% siloxane.[7] However, detailed quantitative data were not presented in their study. Later, Schmitt *et al.*[9] revealed quantitatively that the surface region of 3−5 Å, as measured in ISS, was nearly pure PDMS. Our current results show that the segregation of PDMS to the surface is no greater than 90% even within the topmost 18 Å layer of the BPAC−PDMS (35/65) random block copolymer. This is may be due to the relatively short PDMS blocks in the BPAC−PDMS. Since PDMS and BPAC are covalently linked in the copolymer, BPAC blocks would move along with PDMS as the latter migrates and enriches in the surface region. The concomitant movement of BPAC blocks may cause PDMS blocks from forming a pure PDMS layer at the surface. Previous studies[5] of short block length PDMS copolymers showed a similar result. Chen *et al.*[20] have systematically studied block length effects of this sort:

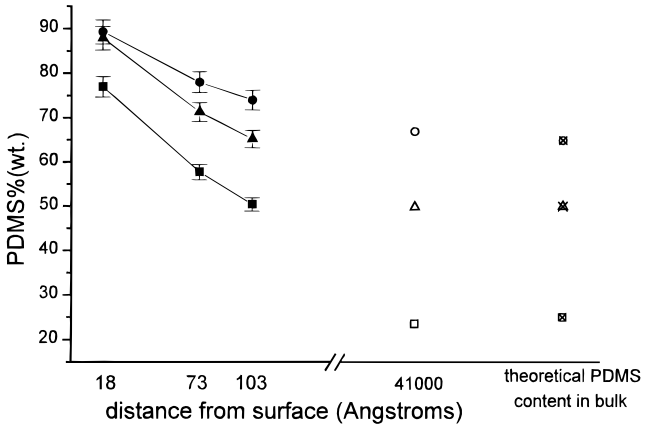

Figure 6. PDMS concentrations for the BPAC−PDMS copolymers cast from chloroform as measured by ESCA, 35/65 (●), 50/50 (▲), and 75/25 (■); as measured by ATR-FTIR, 35/65 (○), 50/50 (△), and 75/25 (□); and theoretical values in the bulk, 35/65 (○X), 50/50 (△X), and 75/25 (□X).

examining a series of BPAC−PDMS copolymers (including those reported in the present study) with different block lengths. Figure 5 also indicates that the surface concentration of PDMS increases with increasing PDMS content in the bulk and the degree of surface enrichment of PDMS varies with different compositional BPAC−PDMS copolymers; of them the BPAC−PDMS (75/25) has the highest degree of PDMS enrichment, 50/50 the second highest, and 35/65 the least. In other words, a copolymer of higher PDMS concentrations leads to a higher absolute PDMS surface concentration, but, does not necessarily result in a higher degree of PDMS surface enrichment. This is consistent with Schmitt's[5,9] and Chen's[20] previous results.

Concentration Gradient in the Near Surface Regions. Figure 6 is a comparison of the weight percentage PDMS at varying depths of the BPAC−PDMS copolymers cast from chloroform, along with the PDMS bulk contents. The concentrations of PDMS are average values over sampling depths of 18, 73, and 103 Å and 4.1 μm. It is clear that these values change progressively from the free surface to the bulk with PDMS at a higher percentage in the surface regions than that in the bulk. The surface concentrations of PDMS measured by ESCA at all sampling depths, up to 100 Å, are significantly higher than their bulk counterparts. The PDMS concentrations in the 4.1 μm regions as measured in ATR-FTIR are nearly identical to the bulk values. In addition, the degree of PDMS surface enrichment would decreases with increasing PDMS content in the bulk, and it also depends on casting solvents (to be detailed later). In fact, LeGrand[30] has proposed a morphology model to describe the morphology of this type of BPAC−PDMS random block copolymers, stating that small BPAC domains are separated by a continuous matrix containing both PDMS and BPAC components in the bulk with the surface region composed of a PDMS-rich phase.

Solvent Solubility Effect on Surface Segregation. Besides the strong compositional dependence, the morphology of the BPAC−PDMS block copolymers is also substantially dependent upon the solvent from which the sample is cast. It is believed that the solvent, during casting, may provide the needed chain mobility through plasticization, permitting the air−polymer interface to attain a favorably low interfacial energy.

Of those six solvents used, carbon tetrachloride is the poorest one for the BPAC−PDMS copolymer. The

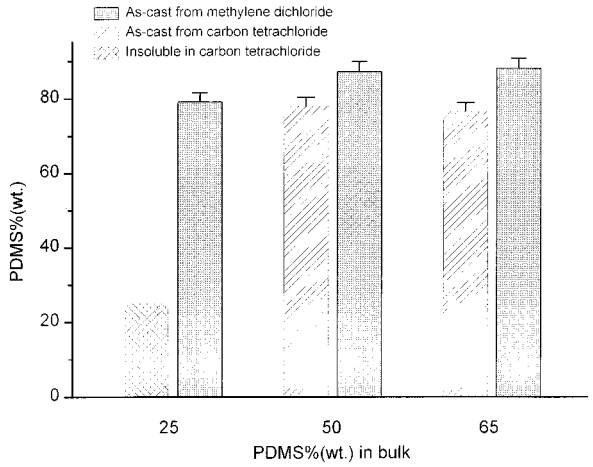

Figure 7. Solubility effect on the PDMS surface (in the topmost 18 Å) concentration of the BPAC−PDMS copolymers.

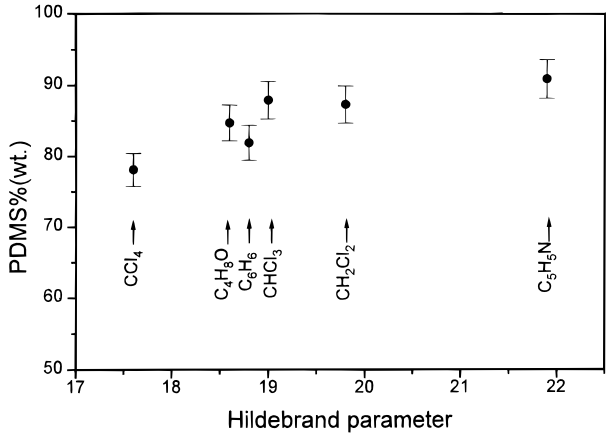

Figure 8. Correlation between the PDMS surface (in the topmost 18 Å) enrichment of the BPAC−PDMS (50/50) copolymer and the solvent Hildebrand parameter.

higher the content of BPAC in the BPAC−PDMS copolymer, the poorer the solubility of the copolymer in carbon tetrachloride, so much so that carbon tetrachloride could not dissolve the BPAC−PDMS (75/25) copolymer having the highest BPAC content. In other words, interactions of the polymer chains with carbon tetrachloride are not as strong as with other solvents. Consequently, the polymer chains in carbon tetrachloride tend to contract instead of stretching. It is less likely for PDMS blocks in such conformations to migrate toward the surface, forming a lower energy surface with excessive PDMS at the surface. It is not surprising that the degree of surface segregation of PDMS in the topmost 18 Å, for instance, is less for films cast with carbon tetrachloride than, for example, for those cast with methylene dichloride (see Figure 7).

Figure 8 shows a correlation between the degrees of PDMS segregation in the topmost 18 Å of the BPAC−PDMS (50/50) copolymers and Hildebrand parameters of solvents. In general, it appears that the surface concentration of PDMS increases with increasing solvent Hildebrand parameter value from carbon tetrachloride to pyridine. However, the surface concentration of PDMS for the sample cast with THF is noticeably higher than that with benzene. This may be explained by the fact that only dispersive and polar solubility terms for solvents are considered in Hildebrand parameter[31] regardless of hydrogen bonding forces. These cannot be ignored for a solvent such as tetrahydrofuran (THF). The Hildebrand parameter (18.6 $MPa^{1/2}$) of THF

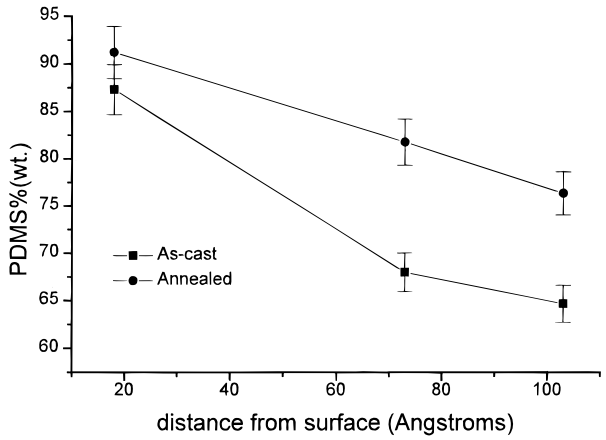

Figure 9. Annealing effect on the surface segregation of the BPAC−PDMS (50/50) copolymer cast from methylene dichloride by ESCA measurements.

is less than that of benzene (18.8 $MPa^{1/2}$), but hydrogen bonding terms (δ_h) of THF (8.0 $MPa^{1/2}$)[31] is much greater than that of benzene (2.0 $MPa^{1/2}$);[31] the overall solubility of BPAC−PDMS in THF is actually better than in benzene.

Annealing Effect on Surface Segregation. As the solvent evaporates, a polymer segment in an increasingly concentrated solution enjoys less and less freedom to move, and even more so as the system getting close to a solid state. Eventually, it would be "frozen", *i.e.*, on a large scale, polymer segment movement is unlikely to occur if the glass transition temperature of either one of the components in a two-component copolymer is sufficiently higher than room temperature. This implies that the surface enrichment of an as-cast film could be less relative to the one having attained thermodynamic equilibrium. Heating such a polymer film above its glass transition temperature annealing could, however, offer polymer chains a driving force to attain a thermodynamic equilibrium, forming a still lower energy surface. Figure 9 illustrates such an annealing effect on the PDMS surface composition of the BPAC−PDMS (50/50) copolymer cast from methylene dichloride. We assert that annealing increases the surface concentration of PDMS remarkably at three different ESCA takeoff angles, and this effect is less pronounced in the topmost region than in the near surface region since that region is nearly saturated (*vide infra*). We have similar observations on the other two types of samples, *i.e.*, the BPAC−PDMS 35/65 and 75/25 copolymers.

When the sampling depth is increased up to 4.1 μm as in ATR-FTIR, the compositions over such regions of the BPAC−PDMS (50/50) copolymer cast from benzene and pyridine are slightly different than the bulk content; in the cases of the other four solvents, however, the compositions are nearly identical to the bulk content, as shown in Figure 10. In addition, Figure 10 shows no significant change of the PDMS surface segregation upon annealing. This may be because annealing treatments only make the polymer segment move locally, affecting the surface layer of much thinner than a couple of micrometers; no morphology change on a large scale occurs.

Solvent Volatility Effect on Surface Segregation. The solvent volatility (or boiling point) varies from solvent to solvent. For example, methylene dichloride has a boiling point of 39.8 °C while pyridine of 115 °C. Thus, it could be predicted that the BPAC−PDMS copolymer films cast with methylene dichloride will be

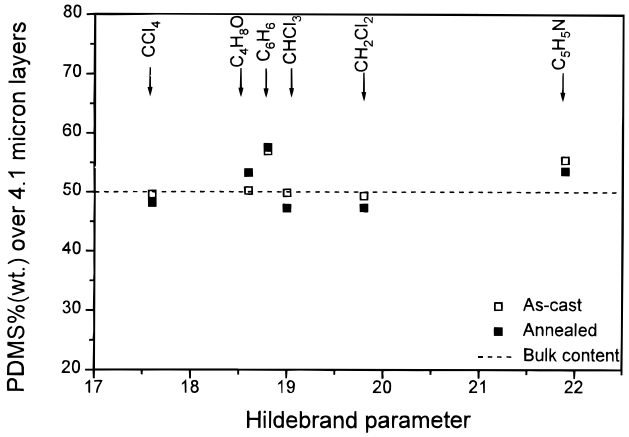

Figure 10. Annealing effect on the segregation of the BPAC−PDMS (50/50) copolymers over the 4.1 μm (from the free surface) layers by ATR-FTIR.

less stable thermodynamically than those with pyridine, because polymer chains in the former case have less time to rearrange themselves into a favorable lower energy state as the solvent evaporates. This proposition can be tested by annealing the as-cast films. As discussed previously, upon annealing a thermodynamically unstable surface, the lower surface energy component-PDMS would be driven further towards the surface, thus more PDMS should be detected. This argument is supported by the results of the BPAC−PDMS (35/65) copolymer cast with methylene dichloride, as shown in Figure 11a. A slight difference is detected, most prominent over the thickest layer. On the other hand, if a surface is already in its thermodynamic equilibrium, the annealing treatment should not be able to change the surface composition. The latter case is exemplified by the results (Figure 11b) of the BPAC−PDMS (35/65) copolymer cast with pyridine having a relative high boiling point. No significant change is detected at any sampling depth in this case.

Solvent "Memory" Effect. An interesting phenomenon is noted when the ESCA data of annealed films are compared. By comparing the absolute concentrations in Figure 11a,b it is evident that annealing the methylene dichloride-cast sample provides a higher concentration of PDMS at the topmost layer of the BPAC−PDMS (35/65) copolymer than the annealed pyridine-cast sample, especially when considering data from the thickest layer (103 Å). We believe this difference may arise from the different morphologies formed from the BPAC−PDMS (35/65) copolymer cast with methylene dichloride and pyridine, respectively. In addition, Figure 12 demonstrates the concentrations of PDMS within the 73 Å thick layers of the annealed BPAC−PDMS (50/50) copolymers cast from the six solvents. The concentrations of PDMS for the copolymer films are not the same even after they were annealed at 180 °C, over 30 °C higher than the highest T_g of the copolymers, for 17 h. Although we are not able to rationalize such differences, we believe that the morphology associated with a certain casting solvent is preserved or "memorized" once formed. As discussed previously, the migrating element in the annealing process (at temperature far below the melting point) is a polymer segment not the entire polymer chain, the large-scale morphology experiences little change while polymer segments undergo local rearrangements. In other words, the structure preservation occurs only in the thick layers as indicated by Figure 12; the compositions of the topmost layers (18 Å thick), as shown in Figure 8, are subject to change upon annealing treatments.

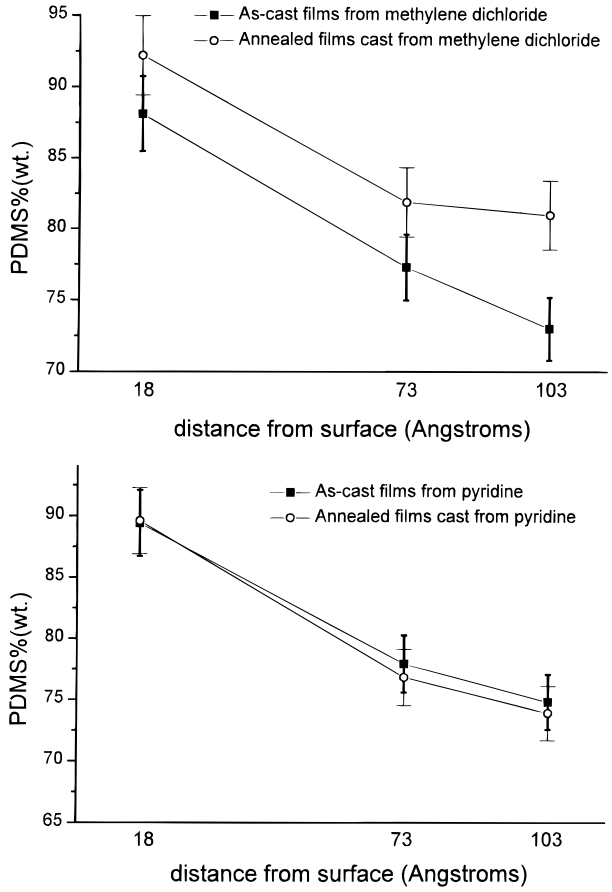

Figure 11. Volatility effect on the kinetics of the film formation: (a) a comparison of PDMS surface concentrations between as-cast films from methylene dichloride and annealed films of the BPAC−PDMS (35/65) copolymer, (b) a comparison of PDMS surface concentrations between as-cast films from pyridine and annealed films of the BPAC−PDMS (35/65) copolymer.

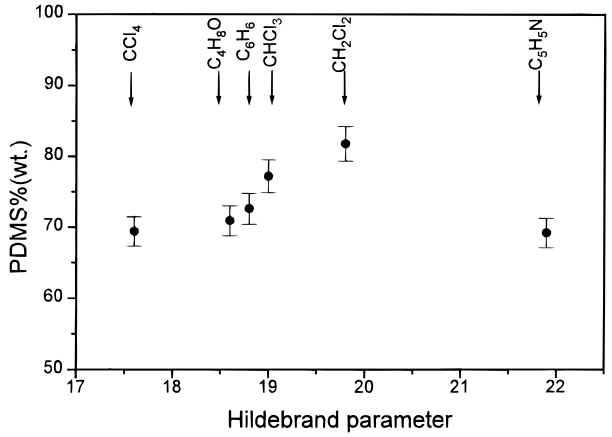

Figure 12. PDMS concentrations in the 73 Å regions of annealed films of the BPAC−PDMS (50/50) copolymer cast from the six solvents.

This so-called solvent "memory" effect can also be seen from the ATR-FTIR results which reflect the compositions in the surface layers of *ca.* 4.1 μm thick. Figure 10 shows no significant difference in PDMS concentrations over 4.1 μm regions between the compositions of a BPAC−PDMS copolymer before and after annealing. Thus, changes due to annealing effect on the scale of

segments—in the range from tens to hundreds of Å—are observed, but not seen at depths probed in ATR-FTIR measurements.

Conclusions

The bulk composition is proven to be an important factor in determining the surface composition and morphology of the random block copolymers of BPAC−PDMS. A major finding of this work is that solvents play a significant role in influencing the surface compositions of those copolymers. The influence varies with the copolymers of different bulk compositions. Generally, the solvent-cast films exhibit surface segregation and concentration gradients of PDMS. Good solvents yield higher PDMS surface concentrations compared to poor solvents. Volatile solvents result in thermodynamically unstable copolymer films. Different solvents lead to peculiar film morphologies, and these morphologies could be preserved once formed. In addition, it is observed that annealing treatments could further enhance the PDMS surface segregation, yet without disturbing the large scale morphology.

Acknowledgment. We are grateful to Dr. R. Kambour from General Electric Co., Schenectady, NY, for the donation of the copolymer samples. This study was financially supported by the Office of U. S. Naval Research, Chemistry and Physics Division, and the National Science Foundation, Polymer Program (Grant DMR-9303032).

References and Notes

(1) Ho, T.; Wynne, K. J. *Macromolecules* **1992**, *25*, 3521.
(2) Clark, D. T.; Peeling, J.; O'Malley, J. M. *J. Polym. Sci., Polym. Chem. Ed.* **1976**, *14*, 543.
(3) Chen, X; Gardella, J. A., Jr.; Kumler, P. L. *Macromolecules* **1992**, *25*, 6621.
(4) Chen, X; Gardella, J. A., Jr. *Macromolecules* **1993**, *26*, 3778.
(5) Schmitt, R. L.; Gardella, J. A., Jr; Magill, J. H.; Chin, R. L. *Polymer* **1987**, *28*, 1462.
(6) Chen, X.; Gardella, J. A., Jr.; Cohen, R. E. *Macromolecules* **1994**, *27*, 2206.
(7) McGrath, J. E.; Dwight, D. W.; Riffle, J. S.; Davidson, T. F.; Webster, D. C.; Viswanathan, R. *Polym. Prepr. (Am. Chem. Soc., Div. Polym. Chem.)* **1979**, *20* (2), 528.
(8) Dwight, D. W.; McGrath, J. E.; Beck, A. R.; Riffle, J. S. *Polym. Prepr. (Am. Chem. Soc., Div. Polym. Chem.)* **1979**, *20* (1), 703.
(9) Schmitt, R. L.; Gardella, J. A., Jr.; Chin, R. L.; Magill, J. H.; Salvati, L., Jr. *Macromolecules* **1985**, *18*, 2675.
(10) Chen, X. Ph. D. Dissertation, Department of Chemistry, State University of New York at Buffalo, NY, 1993.
(11) Chen, X.; Gardella, J. A., Jr. *Macromolecules* **1994**, *27*, 3363.
(12) Grobe, G. L., III; Gardella, J. A., Jr.; Chin, R. L.; Salvati, L., Jr. *Appl. Spectrosc.* **1988**, *42* (6), 989.
(13) Grobe, G. L., III; Nagel, A. S.; Gardella, J. A., Jr.; Chin, R. L.; Salvati, L., Jr. *Appl. Spectrosc.* **1988**, *42* (6), 980.
(14) Chen, X.; Gardella, J. A., Jr.; Ho, T.; Wynne, K. J. *Macromolecules* **1995**, *28*, 1635.
(15) Zhuang, H. Z.; Marra, K. G.; Ho. T.; Chapman, T. M.; Gardella, J. A., Jr. *Macromolecules* **1996**, *29*, 1660.
(16) Gardella, J. A., Jr.; Ho, T.; Wynne, K. J.; Zhuang, H. Z. *J. Colloid Interface Sci.* **1995**, *176*, 277.
(17) Buck, T. M. *Methods of Surface Analysis*; Czanderna, A. W., Ed.; Elsevier: New York, 1975; Chapter 3.
(18) Mittlefehldt, E. R. Ph.D. Dissertation, Department of Chemistry, State University of New York at Buffalo, NY, 1990.
(19) Mittlefehldt, E. R; Gardella, J. A., Jr. *Appl. Spectrosc.* **1989**, *43*, 1173.
(20) Chen, X.; Lee, H. F; Gardella, J. A, Jr. *Macromolecules* **1993**, *26*, 4601.
(21) Seah, M. P.; Dench, W. A. *Surf. Interface Anal.* **1979**, *1* (1), 2.
(22) Perkin-Elmer, *Instruction Manual for 5000 Series ESCA Systems*, Version 2.0.
(23) Harrick, N. J. *Internal Reflection Spectroscopy*; A John Wiley & Sons: New York, 1967; p 30.
(24) Kauppinen, J. K.; Moffatt. D. J.; Mantsch, H. H.; Cameron, D. G. *Anal. Chem.* **1991**, *53*, 1454.
(25) Kauppinen, J. K.; Moffatt. D. J.; Mantsch, H. H.; Cameron, D. G. *Appl. Opt.* **1982**, *21*, 1866.
(26) Kauppinen, J. K. *Appl. Spectrosc.* **1984**, *38*, 778.
(27) DeNoyer, L. K.; Dodd, J. G. *Am. Lab.* **1991**, *23*.
(28) Ferry, A.; Jacobsson, P. *Appl. Spectrosc.* **1995**, *49*, 273.
(29) Zhuang, H. Z. Ph.D. Dissertation, Department of Chemistry, State University of New York at Buffalo, NY, 1996.
(30) LeGrand, D, G. *J. Polym. Sci., Part B: Polym. Phys.* **1969**, *7*, 579.
(31) Brandrup, J.; Immergut, E. H. *Polymer Handbook*, 3rd ed.; John Wiley & Sons: New York, 1989.

MA961138Y